Dynamic resistivity of a two-dimensional electron gas with electric modulation

Godfrey Gumbs
Department of Physics and Astronomy, Hunter College of the City University of New York, 695 Park Avenue, New York, New York 10021, USA

(Received 28 February 2005; revised manuscript received 16 August 2005; published 29 September 2005)

We explore anomalies in the ac transport or produced by electromagnetic wave radiation on the quantum magnetotransport (QMT) coefficients of a two-dimensional electron system (2DES) with electrostatic modulation. An applied magnetic field is perpendicular to the 2DES. The QMT coefficients are determined by the scattering produced by the electrostatic modulation potential, the sub-Landau level eigenstates arising from the formation of new magnetic Brillouin zones, and the ratio of the frequency ω of the electromagnetic radiation to the cyclotron frequency. For strong modulation, it is found that the Hall resistivity $\rho_{xy}(\omega)$ is quenched and becomes negative for low magnetic fields. The magnetic field range over which $\rho_{xy}(\omega)$ is quenched and negative increases as the frequency is increased. The longitudinal resistivity $\rho_{xx}(\omega)$ has been observed experimentally to have a double peak structure (commensurability of the orbits with the lattice) for strong modulation when $\omega=0$. In the presence of electromagnetic wave excitation, we find that the double peaks are shifted to a higher magnetic field and the resistivity is reduced.

DOI: 10.1103/PhysRevB.72.125342 PACS number(s): 73.23.−b, 72.10.Fk, 73.50.Jt, 03.65.Sq

I. INTRODUCTION

There has recently been a considerable amount of experimental work on the transport properties of the two-dimensional electron system (2DES) when subjected to electromagnetic wave excitation at rf, microwave, and IR frequencies in quantized magnetic fields. In each case, a crucial quantity which plays a key role is the frequency and wave vector-dependent conductivity which is determined by Landau-level transitions. Specifically, we give three examples of the types of measurements which have been performed. The first is related to the observations of some peculiar effects in the 2DES in high mobility GaAs/AlGaAs heterostructures under strong microwave radiation, i.e., the disappearance of the diagonal conductivity without Hall resistance quantization at low temperatures and low magnetic fields.[1] Also, Shubnikov–de Haas–like oscillations in millimeter wave photoconductivity in a high-mobility 2DES were observed in Ref. 2. These giant oscillations in amplitude occur in a weak magnetic field and their period is determined by the ratio of the millimeter wave to the cyclotron frequency. The second example concerns the surface acoustic waves (SAWs) in which the velocity and damping of the SAW depend on the dynamical conductivity of the 2DES.[3] Simon[4] obtained an expression for the velocity shift and the attenuation of the SAW in terms of the frequency and wave-vector-dependent electrical conductivity of the 2DES. The SAW is of relevance in the study of composite fermions for which Halperin, Lee, and Read[5] obtained the nonlocal conductivity at half filling. The third example is the experimental work on 2D edge magnetoplasmons which were studied in the quantum Hall effect (QHE) regime at rf frequencies.[6] There have also been measurements of the microwave photoconductivity of GaAs/AlGaAs heterostructures for which resonant responses were obtained corresponding to a collective plasmon excitations in a perpendicular magnetic field.[7–10] There has been some theoretical work on the oscillations of the components of the conductivity tensor of a 2DES in the presence of microwave radiation.[11] The conductivity of the 2DES at magnetic fields where the usual Shubnikov–de Haas oscillations do not appear was calculated in the semiclassical regime within the framework of the Boltzmann transport equation.

Ever since it became possible to fabricate an array of periodic artificial scatterers in a highly mobile 2DES at the interface of a GaAs/AlGaAs heterostructure,[12–23] many experimentalists have studied the quantum magnetotransport (QMT) properties for a variety of imposed scatterers. This gives rise to a class of effects. For example, for an array of antidots[18,24–26] formed by strong repulsive scatterers embedded in a 2DES, the introduction of spatially modulated 2D potentials leads to dramatic commensurability effects at low magnetic fields and temperatures. As a function of the applied magnetic field, the distinct features in transport experiments are the pronounced resistance peaks[18] (the double peak feature) which are manifest when a cyclotron orbit circumscribes a group of antidots in the square array. However, since the potential barriers forming the antidots are continuously varying functions, the cyclotron orbits are distorted. Noncircular cyclotron orbits have been demonstrated in transport measurements of the cyclotron frequency.[23] In addition, the suppression of the commensurate Weiss oscillations, and the negative and quenched Hall resistivity have been found in a square array of antidots.[18]

Microwave photoconductivity measurements (60–400 GHz) on an antidot array[26] reveal that the resonant signals were shifted to higher magnetic fields with increasing frequency. We supplement the experimental result in Ref. 26 with theoretical calculations of frequency dependence of both transverse and the longitudinal resistivities of antidots. The motivation for revisiting this problem is due to the recent experimental activity exploring anomalies produced by elctromagnetic wave radiation on the QMT coefficients of a 2DES.[1,2] In Refs. 27–29, the effect of radiation on the resistivity was calculated theoretically for a homogeneous 2DES and for the spatially modulated system in a magnetic field.

II. FORMALISM

To investigate the commensurability effects on the frequency-dependent photoconductivity tensor, we use a Kubo-type formula[13,30–33] which we write as a function of frequency ω through $(\mu,\nu=x,y)$

$$L_{\mu\nu}(\omega)=-\frac{ie^2}{2A\omega}\int_{-\infty}^{\infty}d\epsilon\, f_0(\epsilon)\times\mathrm{Tr}[v_\mu\delta(\epsilon-H)v_\nu(\hat{G}^-_{\epsilon+\hbar\omega}-\hat{G}^-_{\epsilon-\hbar\omega})-v_\mu(\hat{G}^+_{\epsilon+\hbar\omega}-\hat{G}^+_{\epsilon-\hbar\omega})v_\nu\delta(\epsilon-H)]. \quad (1)$$

This expression which neglects electron-electron interaction will be sufficient to demonstrate the effects of the lattice scattering. In this notation, A is the sample area, $f_0(\epsilon)$ is the Fermi-Dirac distribution function, the velocity operator is defined as $\mathbf{v}=-(i\hbar\vec{\nabla}-e\mathbf{A})/m^*$ where m^* is the electron effective mass. $\mathbf{A}=(0,Bx,0)$ is the vector potential in the Landau gauge, and $\hat{G}^{\pm}_{\epsilon}=1/(\epsilon-H\pm i0^+)$ are advanced and retarded Green's functions. Here, we neglect the effects from the small current and voltage leads connected to the sample by taking the external electric field as uniform over the whole array. This is justified since the size of a sample used in an experiment is very small compared with the scale over which the electric field varies. Furthermore, we assume that the external electromagnetic field is weak so that the distribution function may be approximated by the Fermi-Dirac function. The results presented here are valid only when the contribution resulting from changes in the electron distribution function can be neglected.[32] Dmitriev *et al.*[33] discussed in detail the relationship between the conductivity of a 2DES subjected to a magnetic field and a random potential. They used their calculations based on Eq. (1) to explain the experimental results of Mani *et al.*[1] and Zudov *et al.*[2] for the measured photoconductivity. Durst *et al.*[28] also used the Kubo formula in their calculations of photoconductivity.

In a high mobility sample, and assuming a weak impurity scattering potential, we may separate the contributions to $L_{\mu\nu}(\omega)$ from the subbands and a part arising from electron-impurity scattering. In our numerical calculations, we treat the scattering as being mainly due to the lattice which, after a calculation using Eq. (1), yields the following expressions for the longitudinal and transverse conductivity:

$$L_{\mathrm{xx}}(\omega)=L_{\mathrm{yy}}(\omega)=\frac{\pi e^2\hbar^2\Phi N_y}{\omega m^{*2}A}\sum_{j,j'}\int_{-Gl_H^2/2}^{Gl_H^2/2}\frac{dX_0}{a}(F^{(2)}_{j,X_0;j',X_0})^2\times\int_{-\infty}^{\infty}d\epsilon\, D_{j',X_0}(\epsilon)\{[f_0(\epsilon-\hbar\omega)-f_0(\epsilon)]\times D_{j,X_0}(\epsilon-\hbar\omega)-[f_0(\epsilon+\hbar\omega)-f_0(\epsilon)]\times D_{j,X_0}(\epsilon+\hbar\omega)\}, \quad (2)$$

$$L_{\mathrm{yx}}(\omega)=-L_{\mathrm{xy}}(\omega)=\frac{4e^2\hbar^3\Phi N_y}{m^{*2}A}{\sum_{j,j'}}'\int_{-Gl_H^2/2}^{Gl_H^2/2}\frac{dX_0}{a}\times\frac{1}{[\epsilon_j(X_0)-\epsilon_{j'}(X_0)]^2-(\hbar\omega)^2}\times\left[\frac{1}{l_H^2}\mathrm{Re}(F^{(1)}_{j,X_0;j',X_0}F^{(2)}_{j',X_0;j,X_0})+\mathrm{Im}(F^{(3)}_{j,X_0;j',X_0}F^{(2)}_{j',X_0;j,X_0})\right]\times\int_{-\infty}^{\infty}d\epsilon D_{j,X_0}(\epsilon)f_0(\epsilon). \quad (3)$$

In the above equation the summation with the prime means that all terms with $|\epsilon_j(X_0)-\epsilon_{j'}(X_0)|=\hbar\omega$ must be excluded and $\epsilon_j(X_0)$ are the energy eigenvalues of the electrons in a lattice with period a. Also, $G=2\pi/a$ is a reciprocal lattice vector, $L_y=N_ya$ is the sample length in the y direction, $X_0=k_yl_{\mathrm{H}}^2$ is the guiding center, $l_{\mathrm{H}}=\sqrt{\hbar/eB}$ is the magnetic length, and k_y is a wave vector along the y direction. The normalized magnetic flux is denoted by $\Phi=Ba^2/\phi_0$, where $\phi_0=h/e$ is the flux quantum and the partial density-of-states is $D_{j,X_0}(E)=\delta[E-\epsilon_j(X_0)]$. Here, the structure factors determining the group velocities are

$$F^{(1)}_{j,X_0;j',X_0}=F^{(1)}_{j',X_0;j,X_0}=\int_A d\mathbf{r}\;\psi^*_{j,X_0}(\mathbf{r})x\psi_{j',X_0}(\mathbf{r}),$$

$$F^{(2)}_{j,X_0;j',X_0}=-F^{(2)}_{j',X_0;j,X_0}=\int_A d\mathbf{r}\;\psi^*_{j,X_0}(\mathbf{r})(\partial/\partial x)\psi_{j',X_0}(\mathbf{r}),$$

$$F^{(3)}_{j,X_0;j',X_0}=F^{(3)}_{j',X_0;j,X_0}=-i\int_A d\mathbf{r}\;\psi^*_{j,X_0}(\mathbf{r})(\partial/\partial y)\psi_{j',X_0}(\mathbf{r}),$$

where $\psi_{j,X_0}(\mathbf{r})$ are the eigenfunctions.[34] In the Appendix, we quote the corrections to $L_{\mu\nu}(\omega)$ arising from electron-impurity scattering.

The lattice potential $U_{\mathrm{L}}(\mathbf{r})$ for the scatterers can be taken as having the following form:[34,35]

$$U_{\mathrm{L}}(\mathbf{r})=V_0\left[\cos\left(\frac{2\pi x}{a}\right)\cos\left(\frac{2\pi y}{a}\right)\right]^{2N}, \quad (4)$$

where V_0 is either a positive (or negative) amplitude for the quantum antidot (or dot) regime of the artificially imposed positive (or negative) periodic modulation potential, N is the power for determining the size of the quantum antidot (or dot) potential. We will introduce a dimensionless quantity $\bar{V}_0=m^*V_0a^2/2^{1/2}\pi\hbar^2$. The reason for taking $2N$ as an exponent is to ensure a positive (or negative) potential when $\bar{V}_0$ is taken as a positive (or negative) value. The value of N describes the gradient or degree of modulation of the potential. Equation (4) has been used to simulate antidots[35] when N is large $(N\sim 10)$. One of the reasons we are interested in this potential is that we can adjust both the strength of the potential $\bar{V}_0$ as well as the steepness of the modulation potential by

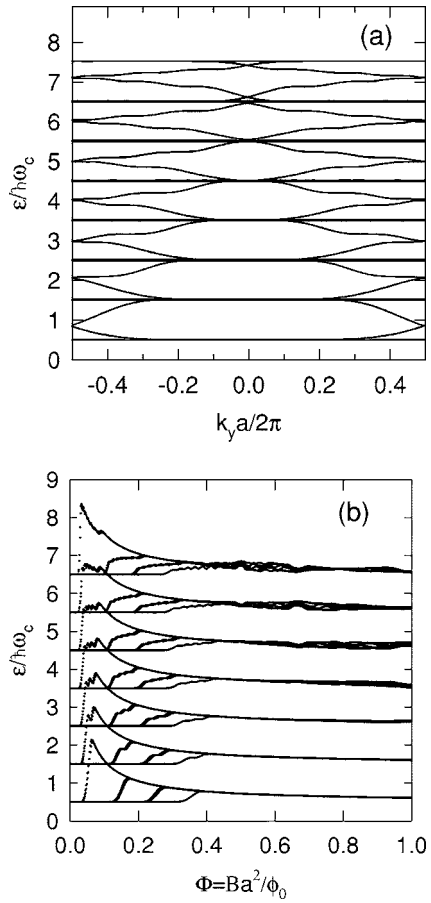

FIG. 1. (a) The energy eigenvalues as functions of $k_y a$ for $\Phi=0.15$, $\bar{V}_0=1.23$. (b) For $k_y a=\pi$, the eigenvalues are plotted as functions of Φ when $\bar{V}_0=5.0$. The parameters used in the calculation are given in the text.

suitably choosing the $2N$ power. We now present numerical results for the longitudinal and transverse resistivities for an array of antidots in the absence and presence of electromagnetic wave radiation. The experimental measurements of the Hall and longitudinal resistivity were carried out on samples of high mobility. Consequently, it is reasonable to exclude impurities as the cause of the observed effects. In the low magnetic field regime, many-particle interactions are known not to give rise to any peculiarities in the magnetotransport coefficients for a homogeneous 2D electron gas. Thus, the Coulomb interactions between electrons will be neglected. Consequently, we will only calculate numerically the band part of the conductivity, since the impurity scattering is weak compared with the lattice scattering. As a matter of fact, the contribution to the resistivity due to electron-impurity effects to leading order does not significantly affect our results.

III. NUMERICAL RESULTS AND DISCUSSION

In Figs. 1(a) and 1(b), we have plotted the energy eigenvalues as a function of the wave vector k_y for $N=10$ in the scattering potential in Eq. (4) (see Ref. 34 for details of the calculation). The dispersion becomes more significant with increasing subband level. As Φ is reduced (to $\Phi\approx 0.05$),

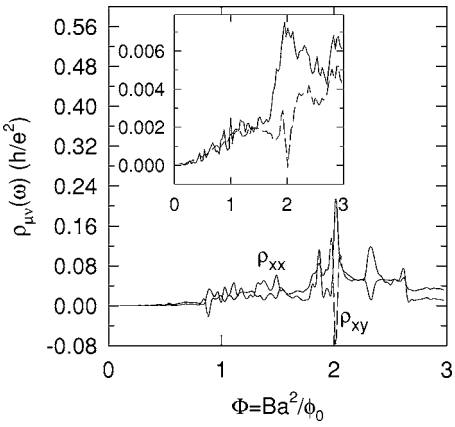

FIG. 2. The longitudinal (solid line) and Hall resistivity (dashed line) at $T=0$ K as a function of the flux Φ in units of the flux quantum $\phi_0=h/e$ for $n_{2D}a^2=1$, $N=10$, $\hbar\omega=E_F$ and $\bar{V}_0=1.23$. In the inset, we chose $\omega=0$ and all other parameters the same.

there is little dispersion near the center of the Brillouin zone. For negative $\bar{V}_0$, the energy eigenvalues could be negative. Figure 1(b) shows the dependence of the energy eigenvalues as a function of magnetic flux for a chosen strength of scattering potential. Here, we chose $k_y a=\pi$, $N=10$, and $\bar{V}_0=5.0$. When the magnetic field is weak, there are large band width oscillations as a function of magnetic field. Although there is no overlap between different Landau levels for weak scattering, our calculations show that the coupling between Landau eigenstates cannot be ignored. This can be deduced from the expansion coefficients for the eigenfunctions which are obtained by numerical diagonalization of the coefficient matrix.[34] This coupling leads to substantial modification of the group velocities. When the lattice potential is increased, the energy levels are shifted upward at low magnetic fields and the band width oscillations are greatly suppressed as shown in Fig. 1(b). When the lattice scattering is further increased, the Landau levels overlap at low magnetic fields.

In Figs. 2 and 3, we plot the longitudinal and transverse Hall resistivity as functions of Φ for two values of $\bar{V}_0$ and ω with $n_{2D}a^2=1$, where n_{2D} is the areal electron density. The magnetoresistance is calculated from the tensor inversion of Eqs. (2) and (3). At low magnetic fields, when $\bar{V}_0$ is in-

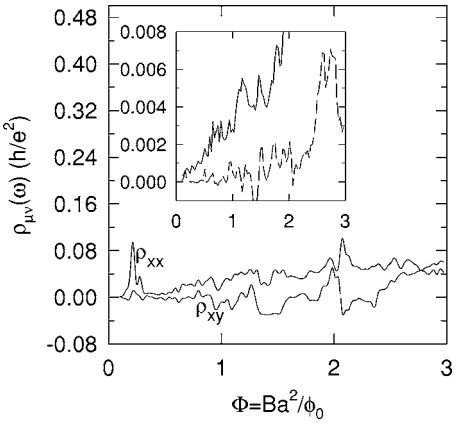

FIG. 3. The same as Fig. 2 except that $\bar{V}_0=100.0$.

creased, large-amplitude, plus-to-minus oscillations are produced in $\rho_{xy}(\omega)$ for $\Phi \leqslant \Phi_{th}$, where Φ_{th} is a threshold where the cyclotron radius is small compared to the lattice spacing and the system behaves like a homogeneous 2DES. The behavior at low Φ is a result of the strong mixing of the Landau levels and the Landau orbits with different guiding centers when $\bar{V}_0$ is large. A negative $\rho_{xy}(\omega)$ occurs when electrons are scattered resonantly from the periodic lattice of scatterers. At these values of Φ, the net scattering force overbalances the Lorentz force. However, these large-amplitude oscillations are suppressed when Φ is increased. At large electron density, the peaks for $\rho_{xy}(\omega)$ are shifted to large magnetic fields.

Figure 2 shows that when the modulation strength is decreased, the double peak (commensurability) structure at a low magnetic field in the longitudinal resistivity is suppressed. As Fig. 3 indicates, when the modulation potential is strong, the effect of finite frequency is to enhance the double peaks, corresponding to the reduced mobility at low B. When Φ decreases, there is a quenching and negative value of ρ_{xy}, as observed experimentally at zero frequency. Our results show that we also have quenching at finite frequency and that as seen in Fig. 2, the quenching and negative resistivity occur for larger Φ when the frequency is increased. The obtained results also indicate that the effect of finite frequency for weak modulation on ρ_{xx} is to produce a suppression of the magnetoresistivity over a range of magnetic fields where ρ_{xy} is quenched. Comparing our results, we find that larger $\bar{V}_0$ causes ρ_{xy} to decrease in magnitude for large Φ. The longitudinal resistivity is decreased as the frequency is increased for either weak or strong modulation. This means that the lattice enhances the forward scattering of electrons at low magnetic fields in the presence of electromagnetic excitation. Our calculations also show that as n_{2D} is increased, Φ_{th} becomes large and the negative ρ_{xy} is greatly reduced. For $\Phi \leqslant \Phi_{th}$, the negative peaks in ρ_{xy} are determined by the collimated states with $\sigma_{xy} \lesssim 0$.

IV. CONCLUDING REMARKS

In summary, we have calculated the Hall and longitudinal resistivities for a 2DES with electrostatic modulation in the classical low magnetic field regime. The experimental results in Ref. 26 showed how ρ_{xx} is affected at microwave frequencies. Our results qualitatively agree with these results. In addition, we demonstrated how the quenching of the Hall effect as well as the related anomalous peaks in the longitudinal resistivity within the quenching regime for a square array of scatterers could be affected by the presence of electromagnetic excitation. Our results clearly demonstrate the effect of finite frequency on forward scattering which increases the conductivity.

In this paper, we did not consider the nonequilibrium or nonlinear collective excitation effects on the electron transport in the 2DES. Such effects were included in some of the quoted references in the text. For example, Dietel *et al.*[29] presented a detailed calculation of the microwave photoconductivity of a 2DES in the presence of a static periodic potential. These authors found that the combination of this potential, a perpendicular magnetic field and the microwave radiation may give rise to an anisotropic negative conductivity of the 2DES which they attribute to nonlinear excitation effects. Also, it was shown by Dmitriev *et al.*[32,33] that the ac conductivity can be used to describe nonlinear effects. In the present paper, no such nonlinear effects were included in our calculations. An equilibrium Green's function approach was used and the negative resistivity which we report arises from backscattering off the lattice. We hope that this study will stimulate experiments to verify our predictions.

ACKNOWLEDGMENT

We acknowledge partial support from the National Science Foundation under Grant No. CREST 0206162 and PSC-CUNY Grant No. 65485-00-34.

APPENDIX: EFFECT DUE TO IMPURITY SCATTERING

In this appendix, we quote the results for the corrections to the conductivity arising from electron-impurity scattering. We have at frequency ω

$$\delta L_{\mu\nu}(\omega) = -\frac{e^2}{4\pi\omega A}\sum_{M,N} v_\mu^{MN} v_\nu^{NM} \int_{-\infty}^{\infty} d\epsilon f_0(\epsilon) \times \{\Delta G^0_{\epsilon,N}[G^{0+2}_{\epsilon+\hbar\omega,M}\Sigma^+(\epsilon+\hbar\omega) - G^{0+2}_{\epsilon-\hbar\omega,M}\Sigma^+(\epsilon-\hbar\omega)]$$
$$+ [\Delta G^0_{\epsilon+\hbar\omega,N} - \Delta G^0_{\epsilon-\hbar\omega,N}]G^{0+2}_{\epsilon,M}\Sigma^+(\epsilon) - \Delta G^0_{\epsilon,M}[G^{0-2}_{\epsilon+\hbar\omega,N}\Sigma^-(\epsilon+\hbar\omega) - G^{0-2}_{\epsilon-\hbar\omega,M}\Sigma^-(\epsilon-\hbar\omega)]$$
$$- [\Delta G^0_{\epsilon+\hbar\omega,M} - \Delta G^0_{\epsilon-\hbar\omega,M}]G^{0-2}_{\epsilon,N}\Sigma^-(\epsilon)\}, \tag{A1}$$

where $G^{0\pm}_{\epsilon,M} = 1/(\epsilon - \epsilon_M \pm i\eta)$ and $v_\mu^{MN} = \langle M|v_\mu|N\rangle$ is a velocity matrix element for eigenstates $|M\rangle$ and $|N\rangle$. Also, $\Delta G^0_{\epsilon,M} = G^{0+}_{\epsilon,M} - G^{0-}_{\epsilon,M}$

If we assume that the distribution of the impurities is not dense and uncorrelated,[21] the scattering potential is short ranged due to screening by the electrons,[4,10,21] and the self-energy is independent of all quantum numbers.[4,10] In this limit, we can easily include impurity scattering effects and obtain the self-consistent equation for the self-energy, i.e.,

$$\Sigma^{\pm}(E) = \frac{2\pi\hbar^2 u_0 n_I}{m^*}\left[1 - \frac{2\pi\hbar^2 u_0 N_y \Phi}{m^* A}\sum_j \int_{-Gl_H^2/2}^{Gl_H^2/2} \frac{dX_0}{a}\left(\frac{1}{E \pm i\eta - E_j(X_0) - \Sigma^{\pm}(E)}\right)\right]^{-1}, \tag{A2}$$

where n_I is the impurity density and u_0 is an impurity scattering amplitude. In this result, one includes multiple scattering from a single scatterer self-consistently. Since $\delta L_{\mu\nu} \sim \Sigma$, we neglect it for the low impurity concentration n_I and the weak electron-impurity scattering compared with the lattice potential, i.e., $u_0 \ll V_0$.

[1] R. G. Mani, J. H. Smet, K. von Klitzing, V. Narayanamuru, and V. Umansky, Nature (London) **420**, 646 (2002).

[2] M. A. Zudov, R. R. Du, J. A. Simmons, and J. L. Reno, Phys. Rev. B **64**, 201311(R) (2001); M. A. Zudov, R. R. Du, L. N. Pfeiffer, and K. W. West, Phys. Rev. Lett. **90**, 046807 (2003).

[3] M. A. Paalanen, R. L. Willett, P. B. Littlewood, R. R. Ruel, K. W. West, L. N. Pfeiffer, and D. J. Bishop, Phys. Rev. B **45**, 11342 (1992).

[4] S. H. Simon, Phys. Rev. B **54**, 13878 (1996).

[5] B. I. Halperin, P. A. Lee, and N. Read, Phys. Rev. B **47**, 7312 (1993).

[6] V. I. Talyanskii, D. R. Mace, M. Y. Simmons, M. Pepper, A. C. Churchill, J. E. F. Frost, D. A. Ritchie, and G. A. C. Jones, J. Phys.: Condens. Matter **7**, L435 (1995); V. I. Talyanskii, J. E. F. Frost, M. Pepper, D. A. Ritchie, M. Grimshaw, and G. A. C. Jones, J. Phys.: Condens. Matter **5**, 7643 (1993).

[7] E. Vasiliadou, G. Muller, D. Heitmann, D. Weiss, K. von Klitzing, H. Nickel, W. Schlapp, and R. Losch, Phys. Rev. B **48**, 17145 (1993).

[8] S. A. Mikhailov and N. A. Savostianova, Phys. Rev. B **71**, 035320 (2005).

[9] J. H. Smet, B. Gorshunov, C. Jiang, L. Pfeiffer, K. West, V. Umanksy, M. Dressel, R. Meisels, F. Kuchar, and K. von Klitzing, Phys. Rev. Lett. **95**, 116804 (2005).

[10] I. V. Kukushkin, J. H. Smet, S. A. Mikhailov, D. V. Kulakovskii, K. von Klitzing, and W. Wegscheider, Phys. Rev. Lett. **90**, 156801 (2003).

[11] A. E. Patrakov and I. I. Lyapilin, J. Low Temp. Phys. **30**, 874 (2004).

[12] D. Weiss, K. von Klitzing, K. Ploog, and G. Weimann, Europhys. Lett. **8**, 179 (1989).

[13] R. R. Gerhardts, D. Weiss, and K. von Klitzing, Phys. Rev. Lett. **62**, 1173 (1989).

[14] R. W. Winkler, J. P. Kotthaus, and K. Ploog, Phys. Rev. Lett. **62**, 1177 (1989).

[15] C. G. Smith, M. Pepper, R. Newbury, H. Ahmed, D. G. Hasko, D. C. Peacock, J. E. F. Frost, D. A. Ritchie, G. A. C. Jones, and G. Hill, J. Phys.: Condens. Matter **2**, 3405 (1990).

[16] K. Ensslin and P. M. Petroff, Phys. Rev. B **41**, 12307 (1990).

[17] R. R. Gerhardts, D. Weiss, and U. Wulf, Phys. Rev. B **43**, 5192 (1991).

[18] D. Weiss, M. L. Roukes, A. Menschig, P. Grambow, K. von Klitzing, and G. Weimann, Phys. Rev. Lett. **66**, 2790 (1991).

[19] A. V. Vagov, Phys. Rev. B **51**, 5065 (1995).

[20] A. Lorke, J. P. Kotthaus, and K. Ploog, Phys. Rev. B **44**, 3447 (1991).

[21] A. Lorke, I. Jejina, and J. P. Kotthaus, Phys. Rev. B **46**, 12845 (1992).

[22] R. Schuster, K. Ensslin, D. Wharam, S. Kühn, J. P. Kotthaus, G. Böhm, W. Klein, G. Tränkle, and G. Weimann, Phys. Rev. B **49**, 8510 (1994).

[23] H. Silberbauer and U. Rössler, Phys. Rev. B **50**, 11911 (1994).

[24] T. Yamashiro, J. Takahara, Y. Takagaki, K. Gamo, S. Namba, S. Takaoka, and K. Murase, Solid State Commun. **79**, 885 (1991).

[25] D. Weiss, K. Richter, A. Menschig, R. Bergmann, H. Schweizer, K. von Klitzing, and G. Weimann, Phys. Rev. Lett. **70**, 4118 (1993).

[26] E. Vasiliadou, R. Fleischmann, D. Weiss, D. Heitmann, K. von Klitzing, T. Geisel, R. Bergmann, H. Schweizer, and C. T. Foxon, Phys. Rev. B **52**, R8658 (1995).

[27] V. Ryzhii, Fiz. Tverd. Tela (Leningrad) **11**, 2577 (1969) [Sov. Phys. Solid State **11**, 2078 (1970)].

[28] Adam C. Durst, Subir Sachdev, N. Read, and S. M. Girvin, Phys. Rev. Lett. **91**, 086803 (2003).

[29] Jrgen Dietel, Leonid I. Glazman, Frank W. J. Hekking, and Felix von Oppen, Phys. Rev. B **71**, 045329 (2005).

[30] Jorgen Rammer, Rev. Mod. Phys. **63**, 781 (1991).

[31] H. U. Baranger and A. D. Stone, Phys. Rev. B **40**, 8169 (1989).

[32] I. A. Dmitriev, M. G. Vavilov, I. L. Aleiner, A. D. Mirlin, and D. G. Polyakov, Phys. Rev. B **71**, 115316 (2005).

[33] I. A. Dmitriev, A. D. Mirlin, and D. G. Polyakov, Phys. Rev. Lett. **91**, 226802 (2003).

[34] G. Gumbs and D. Huang, Superlattices Microstruct. **14**, 1 (1993); Danhong Huang and Godfrey Gumbs, Phys. Rev. B **48**, 2835 (1993).

[35] R. Fleischmann, T. Geisel, and R. Ketzmerick, Phys. Rev. Lett. **68**, 1367 (1992).